EurJIC
European Journal of Inorganic Chemistry

A Journal of ChemPubSoc Europe

Accepted Article

Title: Carbazole as linker for dinuclear gadolinium based MRI Contrast Agents

Authors: BibiMaryam Mousavi, Anne-Sophie Chauvin, Loïck Moriggi, and Lothar Helm

To be cited as: *Eur. J. Inorg. Chem.* 10.1002/ejic.201700847

Link to VoR: http://dx.doi.org/10.1002/ejic.201700847

WILEY-VCH

WILEY-VCH

FULL PAPER

Carbazole as linker for dinuclear gadolinium based MRI Contrast Agents

Bibimaryam Mousavi,[a,b] Anne-Sophie Chauvin,[a] Loïck Moriggi,[a] and Lothar Helm*[a]

Abstract: Ligands able to complex two gadolinium ions have been synthesized and characterized in view of the ability of the complexes to increase spin relaxation of water protons. All ligands are based on the heptadentate DTTA chelator and carbazole as a rigid linker. Depending on the derivatization on the nitrogen atom of the five-membered ring, the compounds form small aggregates in aqueous solution, self-assemble to form micelles or bind to human serum albumin. In all cases, this leads to a marked increase in ^{1}H relaxivity at nuclear Larmor frequencies between 20 and 60 MHz. Water exchange on the gadolinium ions as measured by ^{17}O NMR relaxation is fast enough not to limit relaxivity. ^{1}H nuclear magnetic relaxation dispersion profiles have been measured and analysed using Solomon-Bloembergen-Morgan theory including Lipari-Szabo treatment to include internal motion or anisotropic rotation.

Introduction

In recent years, the number of installed high field MRI scanners working at magnetic fields of 3 T continuously increased. Even if 1.5 T scanners are still the most widely used, the portion of higher field instruments is expected to grow in the next years.[1] This evolution has consequences for the development of contrast agents administered in more than a third of all MRI examinations. Most gadolinium based contrast agents used in clinics have been developed at a time when low field scanners working at 60 MHz or below were mostly installed.[2,3] There is a need for new contrast agents which are adapted for higher magnetic fields and for new application which become feasible with this new instruments.[4–6] Increasing efficiency of MRI contrast agents at low magnetic field is, at least in theory, relatively simple: rotational diffusion and electron spin relaxation have to be slow and exchange of inner sphere water has to be optimal.[3,7–9] At high magnetic field the situation is more complex. Both, rotational diffusion and water exchange have to be optimal; relaxation of the Gd^{3+} electron spin is however of no importance. From theoretical considerations follows that mid-size compounds with rotational correlation times of 0.5 to 1 ns will give best results at magnetic fields above 3 T [5].

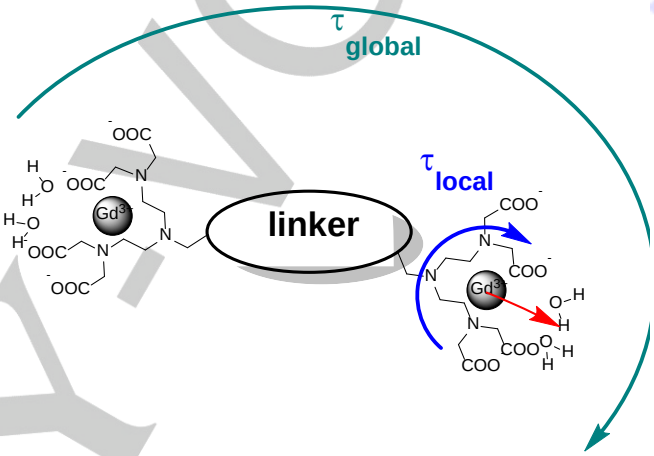

Figure 1. Schematic representation of a dinuclear complex showing global and local rotational diffusion

To achieve a high local enhancement of relaxation it is therefore a good choice to construct relatively small compounds that can accommodate several paramagnetic centres. Examples of such compounds are dinuclear complexes with two Gd^{3+} ions [10–18] (Figure 1) and trinuclear complexes with three Gd^{3+} ions [19–22]. These compounds have rotational correlation times below 1 ns and relaxation enhancement is two to three times higher than on compounds with only one paramagnetic centre. A closer look to the parameters governing relaxivity, the relaxation enhancement per mM of Gd^{3+}, reveals that besides the global rotation of the compound local internal motion can strongly influence the interaction between the ^{1}H nuclear spin of bound water molecules and the spin of the seven unpaired electrons of the lanthanide ion.[8,23,24]

An essential part of di- or in general multinuclear compounds is the linker connecting the chelates bearing the paramagnetic centres (Figure 1). Some linkers used are designed to make the compound responsive for example by its ability to bind cations like Ca^{2+}.[11,12,16,25] Other linkers are hydrophobic organic molecules like benzene or poly-benzene. It has been shown that these compounds tend to form aggregates in aqueous solution, most probably due to interaction between the aromatic rings.[15,18,22] The aggregation leads to longer rotational correlation times and therefore to higher relaxivities mainly in the frequency range between 20 and 80 MHz. These aggregates are very dynamic with fast exchange between monomeric and multimeric species.[18,22] In this situation, a unique rotational correlation time

[a] Institut des Sciences et Ingénieries Chimiques
Ecole Polytechnique Fédérale de Lausanne (EPFL)
1015 Lausanne, Switzerland
E-mail: lothar.helm@epfl.ch
[b] State Key Laboratory of Advanced Technology fort Materials
Synthesis and Processing
Wuhan University of Technology
Wuhan, 430070, PR China

Supporting information for this article is given via a link at the end of the document.

cannot describe the rotational diffusion responsible for the fluctuation of the local magnetic fields.

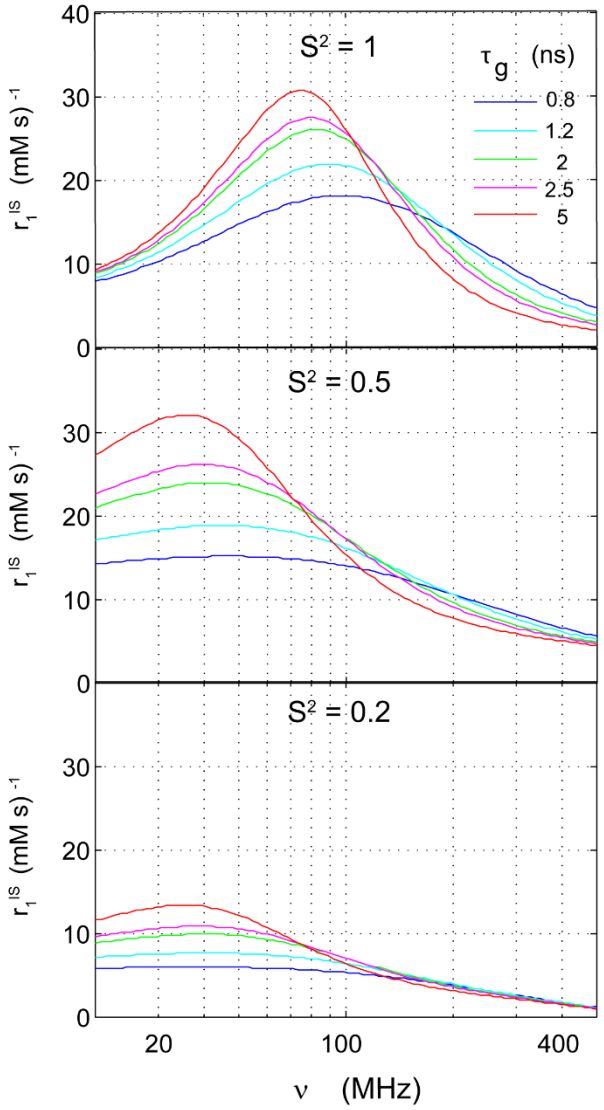

Figure 2. Inner sphere relaxivity r_1^{IS} as a function of the Larmor frequency ν calculated for different global correlation times τ_g and different order parameters S^2 (SBM theory, $k_{ex} = 10^8$ s^{-1}, $\tau_v = 10$ ps, $\Delta^2 = 10^{-19}$ s^{-2}, $r_{GdH} = 3.1$ Å, $\tau_i = 200$ ps).

A simple theoretical description of rotational motion with two characteristic correlation times has been developed by Lipari and Szabo to describe nuclear spin relaxation in macromolecules.[26,27] This so called model free approach has been successfully adapted to describe the rotational behaviour of contrast agents.[28] Adding a local correlation time and an order parameter opens the parameter space but finally does not resolve the problem of relatively low relaxivities at high frequencies (Figure 2). At 400 MHz (9.4 T) for example global correlation times around 1 ns are still optimal. From these simulations, one can see that high order parameters ($S^2 > 0.5$) lead to highest r_1^{IS} values. High order parameters are in general obtained by using rigid linkers or by forming stable densely packed aggregates like micelles.

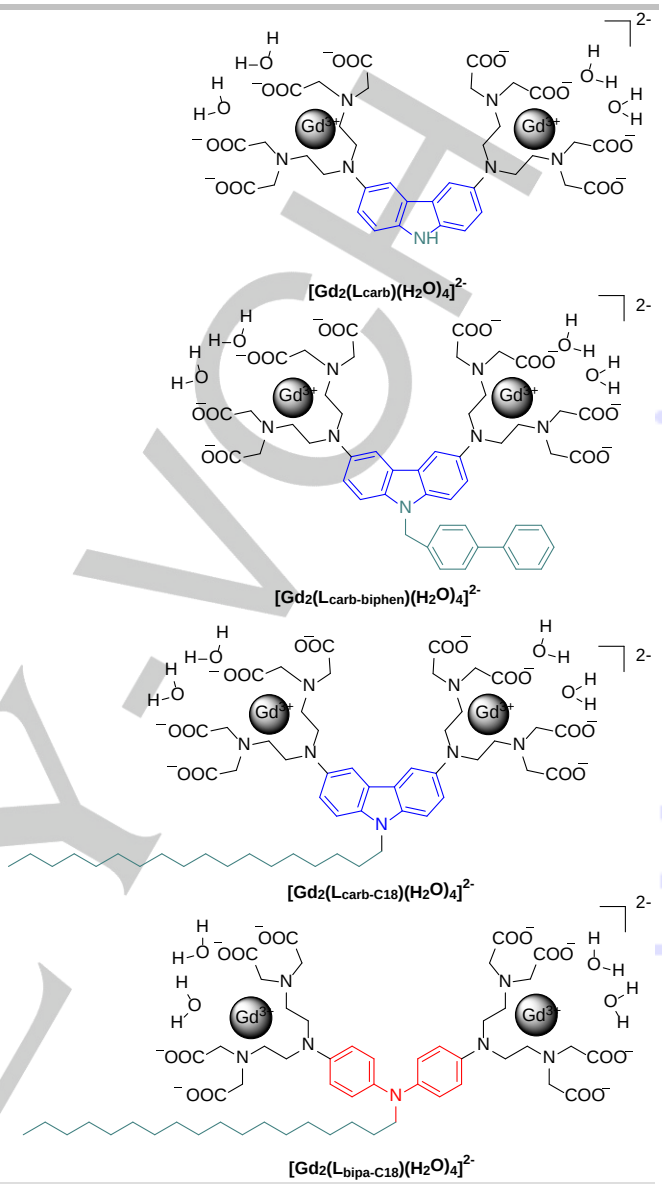

Figure 3. Structures of the gadolinium complexes of this study: $[Gd_2(L_{carb})(H_2O)_4]^{2-}$, $[Gd_2(L_{carb\text{-}biphen})(H_2O)_4]^{2-}$, $[Gd_2(L_{carb\text{-}C18})(H_2O)_4]^{2-}$ and $[Gd_2(L_{bipa\text{-}C18})(H_2O)_4]^{2-}$.

These observations let us to choose a new linker to build dinuclear compounds in view of application as gadolinium based MRI contrast agent. Carbazole is a rigid molecule with the possibility to attach two chelating units to the benzene rings (Figure 3). By attaching the central nitrogen of an acyclic polyaminocarboxylate directly to an aromatic carbon, a relatively high rigidity of the dinuclear compound should be obtained. Carbazole can be further derivatized by adding substituents to the nitrogen atom of the five-membered ring. It is interesting to note that carbazole is also known as chromophore. For example, lanthanide complexes with β-diketonate functionalized carbazoles show interesting photophysical properties which could eventually be exploited using for example Eu^{3+}.[29–32]

Therefore, we have synthetized three ligands in that series: $[Gd_2(L_{carb})(H_2O)_4]^{2-}$ for which the carbazole moiety was attached

to two acyclic polyaminocarboxylate moieties. Addition of substituents on the nitrogen atom of the five-membered ring was also performed. $[Gd_2(L_{carb\text{-}C18})(H_2O)_4]^{2-}$ was designed in order to form aggregates in soluteon and $[Gd_2(L_{carb\text{-}biphen})(H_2O)_4]^{2-}$ in order to bind macromolecules like Human serum albumin (HSA). The last ligand contained a biphenylamine core with a long C18 alkyl chain instead of the carbazole one $[Gd_2(L_{bipa\text{-}C18})(H_2O)_4]^{2-}$, and was synthetized for comparative purposes.

RESULTS

For the synthesis of ligand H_8L_{carb} **6**, 3,6-diaminocarbazole was synthesized in two steps, and subsequently reacted with four equivalents of 2-[*bis*-(*tert*-butyloxycarbonylmethyl)amino] ethylbromide (Figure 4). At this step we could have used protected diethylentriamine; however, using 2-[*bis*-(*tert*-butyloxycarbonyl-methyl)-amino]ethylbromide was preferred to decrease steric problems.

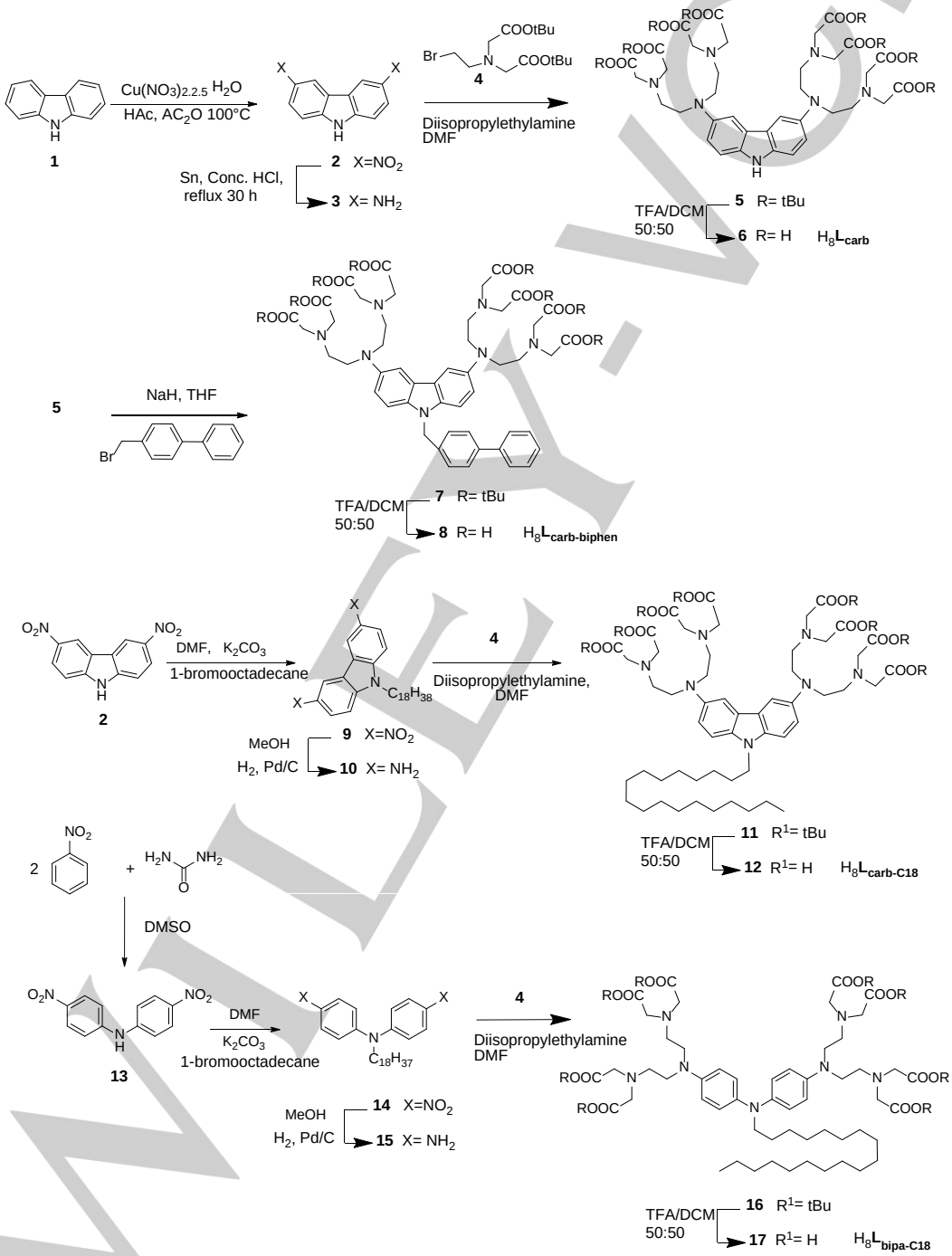

Figure 4. Synthesis of the 4 ligands H_8L_{carb} , $H_8L_{carb\text{-}biphen}$, $H_8L_{carb\text{-}C18}$ and $H_8L_{bipa\text{-}C18}$

For the synthesis of ligand $H_8L_{carb\text{-}biphen}$, compound **5** was reacted with 4-(bromo-methyl) biphenyl using a strong base (NaH) in dry THF. Due to lots of aromatic groups, the purification of this compound was not possible by normal phase chromatography or even using a C18-column in reverse phase chromatography. We prepared a homemade reverse-phase called C3 column which was used for purification. After purification, the *tert*-butyl protecting groups of compounds **5** and **7** were removed by TFA/DCM to give both ligands.

For the synthesis of compound **12**, two different strategies could be used. One was direct reaction of **5** with 1-bromooctadecane using NaH in dry tetrahydrofuran which resulted in a very low 9% yield. Another route was elaborated from carbazole as a starting material. Subsequently, the reaction of **2** with 1-bromooctadecane in DMF using potassium carbonate lead to 3,6-dinitro-9-octadecyl-9H-carbazole **9**. The reduction of the nitro groups of compound **9** to amine groups was performed using palladium on activated charcoal in methanol and compound **10** was obtained. The reduction step followed by reaction of the intermediate **10** with excess 2-[bis-(t-butyloxycarbonylmethyl)-amino]-ethyl-bromide led to compound **11**. The final product **12** was obtained by hydrolysis of the ester precursor with TFA in DCM solvent.

Compound **17** was designed and synthesized to have a similar structure as **12.**

Concentration effect on relaxivity

The more or less hydrophobic linkers are suspected to show aggregation in aqueous solution due to the carbazole itself and due to the attached biphenyl- or C18 groups. The two complexes with carbazole $[Gd_2(L_{carb})(H_2O)_4]^{2-}$ and biphenyl-carbazole $[Gd_2(L_{carb\text{-}biphen})(H_2O)_4]^{2-}$ are suspected to form small aggregates composed of a few monomers.[15,18,22] The compound with C18-carbazole $[Gd_2(L_{carb\text{-}C18})(H_2O)_4]^{2-}$ should be able to form nanosized micelles due to interactions between the long hydrophobic chains.[33] To check for formation of aggregates and micelles in aqueous solution ^{1}H relaxivities have been measured as a function of concentration at 40 MHz and 37 °C. Formation of aggregates should lead to a marked increase in relaxivity at that Larmor frequency due to the increase in rotational correlation time.

The relaxivity of $[Gd_2(L_{carb})(H_2O)_4]^{2-}$ with the two chelates linked to a simple carbazole is nearly independent on concentration up to 4 mM in $[Gd^{3+}]$ (Figure 5). The mean value calculated, r_1 ~ 11.7±0.3 $mM^{-1}s^{-1}$, corresponds to values expected for a monomeric dinuclear compound. This relaxivity is similar to that of $[Gd_2bpy(DTTA)_2(H_2O)_4]^{2-}$ [19] (r_1= 12.4 $mM^{-1}s^{-1}$ at 20 MHz and 37 °C) and higher than r_1 found for other previously studied dinuclear complexes such as $[pip[GdDO3A(H_2O)]_2]$ (r_1= 5.6 mM^{-1} s^{-1}) and $[bisoxa[GdDO3A(H_2O)]_2]$ (r_1= 4.4 mM^{-1} s^{-1}) at 40 MHz and 37 °C [10]. This increase in relaxivity by a factor of two can be explained by the presence of two inner-sphere water molecules in case of the DTTA chelator.

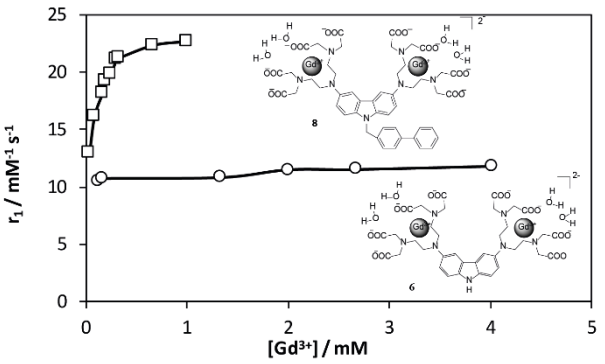

Figure 5. ^{1}H NMR relaxivity as a function of $[Gd^{3+}]$ for $[Gd_2(L_{carb})(H_2O)_4]^{2-}$ (○) and $[Gd_2(L_{carb\text{-}biphen})(H_2O)_4]^{2-}$ (□) (B_0 = 0.94 T; v = 40 MHz; 37°C; $1/T_{1d}$ = 0.37 s^{-1})

In case of $[Gd_2(L_{carb\text{-}biphen})(H_2O)_4]^{2-}$ the relaxivity increases by more than 70% if the concentration of $[Gd^{3+}]$ is raised from 0.033 mM to 1 mM (Figure 5). At low concentration relaxivity is close to that of $[Gd_2(L_{carb})(H_2O)_4]^{2-}$. After a marked increase up to $[Gd^{3+}]$ ~0.7 mM r_1 reaches a plateau with r_1~ 22 mM^{-1} s^{-1}. A simple interpretation of that data is that the monomer of biphenyl-carbazole $[Gd_2(L_{carb\text{-}biphen})(H_2O)_4]^{2-}$ has about the same relaxivity and therefore rotational correlation time as $[Gd_2(L_{carb})(H_2O)_4]^{2-}$. Starting at concentrations of 0.05 mM $[Gd_2(L_{carb\text{-}biphen})(H_2O)_4]^{2-}$ forms aggregates in aqueous solution leading to slower rotational diffusion and therefore higher relaxivities at 40 MHz. The increased hydrophilicity due to the introduction of the biphenyl group is clearly responsible for the formation of aggregates. The increase of r_1 by a factor of about two indicates that the aggregates formed are small comprising two or three monomer units at most.

Complexes $[Gd_2(L_{carb\text{-}C18})(H_2O)_4]^{2-}$ and $[Gd_2(L_{bipa\text{-}C18})(H_2O)_4]^{2-}$ have a long hydrophobic chain attached to the core which will drive the formation of micelles in aqueous solution. The nanosized micelles are formed above a critical micellar concentration, CMC. The formation of micelles leads to slower rotational diffusion of the gadolinium chelates and therefore a marked increase in relaxivity at magnetic fields between 0.5 and 1.5 T.

The biphenyl compound $[Gd_2(L_{bipa\text{-}C18})(H_2O)_4]^{2-}$ shows a marked increase in r_1 at $[Gd^{3+}]$ ~ 0.1 mM (Figure 6). Using equations developed by Nicolle [33] (see ESI) relaxivities of 12 mM^{-1} s^{-1} (below the CMC) and 43 mM^{-1} s^{-1} (above the CMC) are calculated for $[Gd_2(L_{bipa\text{-}C18})(H_2O)_4]^{2-}$. The complex with the carbazole linker $[Gd_2(L_{carb\text{-}C18})(H_2O)_4]^{2-}$ shows high relaxivity already at the lowest concentration measured ($[Gd^{3+}]$ = 0.04 mM, Figure 6). T small change in relaxivity can be assigned to a change in size of the micelles around $[Gd^{3+}]$ = 0.1 mM. The relaxivity plateau with r_1 ~ 46 mM^{-1} s^{-1} is reached at $[Gd^{3+}]$ ~ 0.1 mM. Only an upper limit of the CMC can therefore be given for this compound: CMC < 0.1 mM.

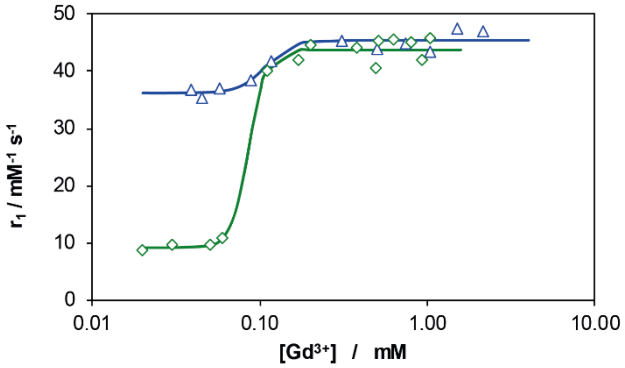

Figure 6. ^{1}H NMR relaxivity as a function of $[Gd^{3+}]$ for $[Gd_2(L_{carb\text{-}C18})(H_2O)_4]^{2-}$ (Δ) and $[Gd_2(L_{bipa\text{-}C18})(H_2O)_4]^{2-}$ (◇); (B_0 = 0.7 T; ν = 30 MHz; 25°C)

^{17}O and ^{1}H NMRD measurements

To obtain detailed information on rotational diffusion behaviour and on water exchange on the carbazole based dinuclear compounds we measured ^{1}H nuclear magnetic relaxation dispersion (NMRD) profiles and ^{17}O transverse relaxation enhancements, $1/T_{2r}$, (Figure 7).

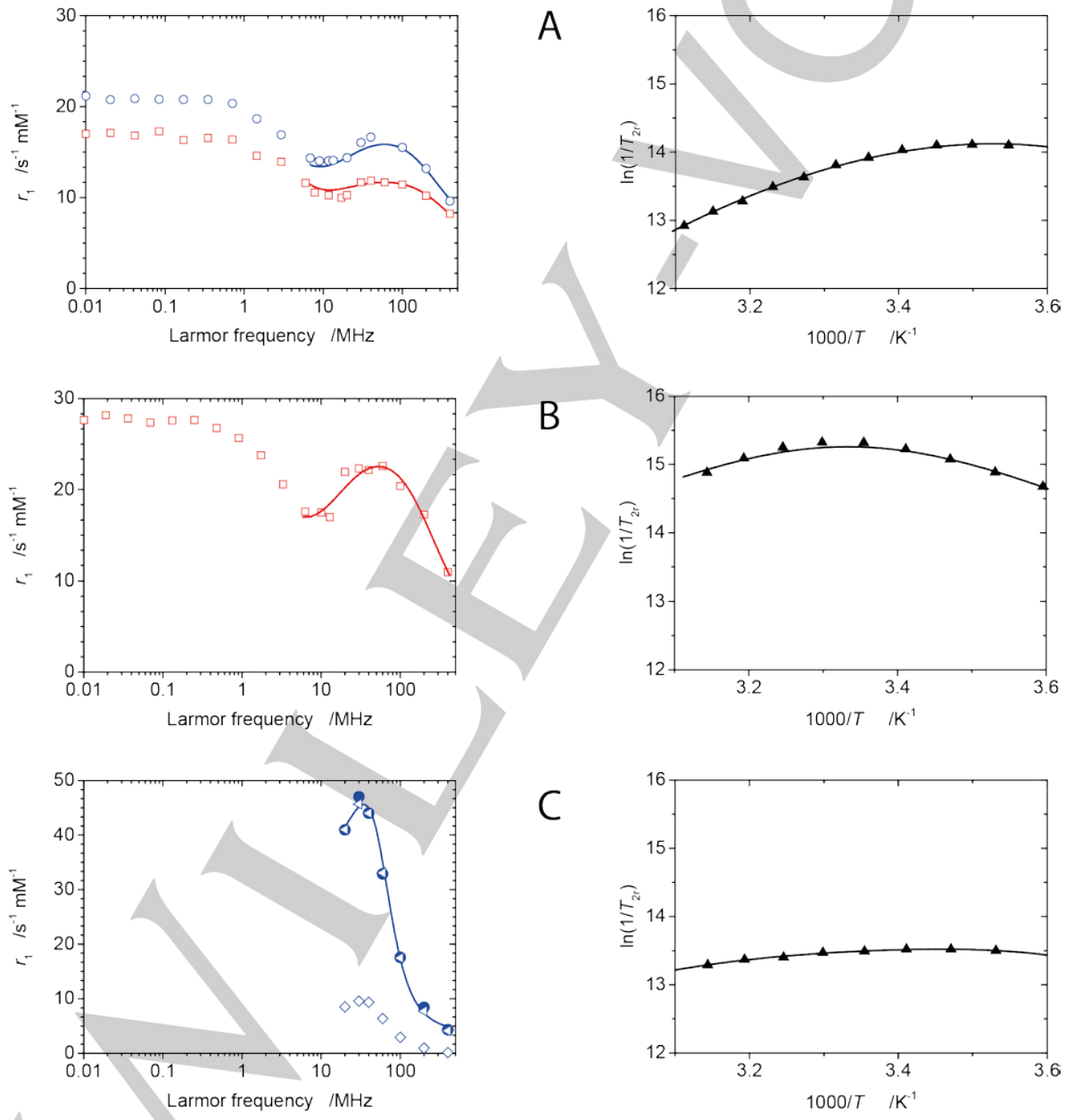

Figure 7 Left: ^{1}H NMRD profiles measured at 25 °C (blue) and 37°C (red); right: ^{17}O transverse relaxation enhancement $1/T_{2r}$ measured at 9.4 T; **A**: $[Gd_2(L_{carb})(H_2O)_4]^{2-}$ $[Gd^{3+}]$ = 4.01 mM; **B**: $[Gd_2(L_{carb\text{-}biphen})(H_2O)_4]^{2-}$ $[Gd^{3+}]$ = 0.66 mM (□), $[Gd^{3+}]$ = 0.58 mM (▲); **C**: $[Gd_2(L_{carb\text{-}C18})(H_2O)_4]^{2-}$ $[Gd^{3+}]$ = 2.16 mM (●), $[Gd^{3+}]$ = 7.09 mM (▲),$[Gd_2(L_{bipa\text{-}C18})(H_2O)_4]^{2-}$ $[Gd^{3+}]$ = 0.62 mM (◁),$[Gd^{3+}]$ = 0.04 mM (◇). The lines correspond to a simultaneous fit of the experimental data points using SBM theory.

The relaxivities of all compounds show a maximum in the MRI relevant frequency region between 20 and 60 MHz (Figure 7, left). The exact position and the highest relaxivity at the maximum depends on electron spin relaxation and on the rotational correlation time.[34] Comparison of the relaxivities in Figure 7 shows that the frequency of the maximum shifts to lower values and the value of r_1 increases by replacing the proton on the carbazole nitrogen by a biphenyl group (B) or by a C18 chain (C). Qualitatively, an increase of the rotational correlation time can be deduced from this data.

The relaxivity curves of both micelle forming compounds, $[Gd_2(L_{carb\text{-}C18})(H_2O)_4]^{2-}$ and $[Gd_2(L_{bipa\text{-}C18})(H_2O)_4]^{2-}$, both measured at concentrations above the CMC, are identical (Figure 7 C, left). This shows that both form micelles of similar size at those concentrations (see ESI for DLS and zeta potentials). The NMRD profile of $[Gd_2(L_{bipa\text{-}C18})(H_2O)_4]^{2-}$ has also been measured for a concentration below the CMC. The maximum of relaxivity is <10 s-1 mM-1, clearly showing the absence of the formation of micelles at that concentration.

Surprisingly, the transverse relaxation rates measured by ^{17}O NMR differ for the three carbazole compounds (Figure 7 right). $1/T_{2r}$ gives direct access to water exchange rate constants, k_{ex}.[35] The chelators used for all dinuclear compounds are all the same, DTTA, and therefore one would expect that water exchange does not differ markedly between the three compounds.

The combined analysis of ^1H NMRD and ^{17}O $1/T_{2r}$ using standard Solomon-Bloembergen-Morgan (SBM) theory together with the Lipari-Szabo approach for anisotropic or internal rotation allowed getting rotational correlation times and water exchange rate constants. (Table 1, for details see ESI). Only relaxivities at Larmor frequencies > 5 MHz have been included in the fit to account for the limited validity of SBM theory.

The water exchange rate constants, k_{ex}^{298}, obtained from the fit (Table 1) confirm the observation made on the experimental data. At 25° C water exchange is three times faster on $[Gd_2(_{Lcarb})(H_2O)_4]^{2-}$ compared to $[Gd_2(L_{carb\text{-}biphen})(H_2O)_4]^{2-}$ and the micellar $[Gd_2(L_{carb\text{-}C18})(H_2O)_4]^{2-}$. One should however keep in mind that the statistical error is relatively big due to strong correlation of the parameters.

Table 1. Best fit parameters of ^1H NMRD and ^{17}O NMR using Solomon-Bloembergen-Morgan theory including Lipari-Szabo approach.

Parameters	$[Gd_2(L_{carb})(H_2O)_4]^{2-}$	$[Gd_2(L_{carb\text{-}biphen})(H_2O)_4]^{2-}$	HSA-$[Gd_2(L_{carb\text{-}biphen})(H_2O)_4]^{2-}$		$[Gd_2(L_{carb\text{-}C18})(H_2O)_4]^{2-}$
	$1/T_2$ ^{17}O, NMRD	$1/T_2$ ^{17}O, NMRD	NMRD, fit A	NMRD, fit B	$1/T_2$ ^{17}O, NMRD
$\Delta H^{\ddagger}$ (kJ mol^{-1})	58 ± 10	35 ± 3	58	36	52 ± 4
$\Delta S^{\ddagger}$ (J K^{-1} mol^{-1})	+90 ± 23	+8 ± 7	-	-	+64 ± 13
k_{ex}^{298} (10^6 s^{-1})	24 ± 12	8 ± 2	24	8	8 ± 3
τ_g^{298} (ps)	725 ± 220	1050 ± 300	3400 ± 460	3100 ± 470	6000 ± 1600
τ_l^{298} (ps)	170 ± 25	360 ± 80	71 ± 11	71 ± 14	75± 10
S^2	0.19 ± 0.09	0.35 ± 0.16	0.28 ± 0.02	0.29 ± 0.02	0.42 ± 0.02

Concerning the rotational motion as characterized by rotational correlation times in all cases two correlation times are necessary to fit the data: a global rotational correlation time τ_g and a local rotational correlation time τ_l (Table 1). The carbazole and the biphenyl-carbazole compounds are characterized by $\tau_g \leq 1$ ns and τ_l of 170 – 350 ps. The main difference in relaxivity comes from the markedly higher order parameter for the aggregate forming biphenyl-carbazole $[Gd_2(L_{carb\text{-}biphen})(H_2O)_4]^{2-}$ (S^2 ~0.35). The micelle forming compound $[Gd_2(L_{carb\text{-}C18})(H_2O)_4]^{2-}$ shows a longer global correlation time τ_g ~ 6 ns but a shorter local one τ_l ~ 75 ps. Again, the order parameter is relatively high, S^2 ~0.4.

$[Gd_2(L_{carb\text{-}biphen})(H_2O)_4]^{2-}$ bound to HSA

Binding of gadolinium based MRI contrast agents to HSA results in a remarkable enhancement in relaxivity in the frequency region of 20 to 80 MHz.[36,37] The ^1H NMRD profiles of a HSA-$[Gd_2(L_{carb\text{-}biphen})(H_2O)_4]^{2-}$ sample is shown in Figure 8 and, as expected, indicates a marked relaxivity hump between 10 and 100 MHz. The ratio of HSA to $[Gd_2(L_{carb\text{-}biphen})(H_2O)_4]^{2-}$ is 3.9 and therefore more than 95% of $[Gd_2(L_{carb\text{-}biphen})(H_2O)_4]^{2-}$ is bound to HSA (for binding constants see ESI). The NMRD profile looks similar to that of HSA-[triphenyl-[Gd(DOTMA)(H_2O)]$^-$] [38] which possesses a similar HSA binding site. The relaxivity increases if the temperature is lowered indicating that water exchange is not limiting relaxivity in this case. No ^{17}O NMR study could be performed due to the very low concentration of gadolinium in the sample.

The NMRD profiles have been fitted neglecting the small amount of unbound complex and using water exchange parameters from $[Gd_2(_{Lcarb})(H_2O)_4]^{2-}$ (fit A) or from $[Gd_2(L_{carb\text{-}biphen})(H_2O)_4]^{2-}$ (fit B, see Table 1). The correlation times and the order parameter fitted change only within less than one standard deviation confirming that water exchange is not limiting relaxivity. The global rotational correlation time τ_g ~3-4 ns is of the order of that of micelles.[39] The HSA-$[Gd_2(L_{carb\text{-}biphen})(H_2O)_4]^{2-}$ construct has however a lower order parameter compared to that of the micelles.

WILEY-VCH
10.1002/ejic.201700847

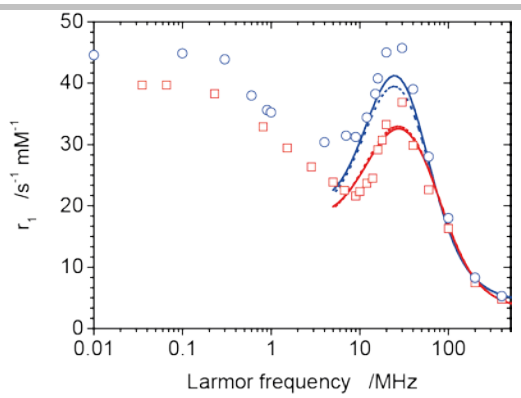

Figure 8. ^{1}H nuclear magnetic relaxation dispersion profiles of HSA-$[Gd_2(L_{carb\text{-}biphen})(H_2O)_4]^{2-}$ ($[Gd^{3+}]$=77 μM) at 25 °C (○) and 37 °C (□). The lines represent the simultaneous least squares fit of points above 6 MHz (full line: fit A, dashed line: fit B, Table 1).

DISCUSSION

Water exchange rate constants have now been measured on a series of gadolinium chelates with the heptadentate DTTA chelator. Most of the k_{ex}^{298} values measured are around $8{\cdot}10^6$ s^{-1} (see Table 2). Three compounds show an up to three times faster water exchange, namely the monomer $[Gd(DTTA\text{-}Me)(H_2O)]^-$ [40], the dimer $[Gd_2(L_{carb})(H_2O)_4]^{2-}$ and the tetramer $\{Ph_4[Gd(DTTA)(H_2O)_2]^-{}_3\}$ [22]. The reason for this change in water exchange is unclear. All exchange rate constants have been measured by ^{17}O NMR The charge of the Gd-DTTA units is -1 and the substitution is in all cases at the central nitrogen of the DTTA. A dissociative activation mode should operate in all cases as can be seen from the positive activation entropies and the activation volume $\Delta V^{\ddagger}$ of +8 cm^3 mol^{-1} measured for water exchange on $[Gd(DTTA\text{-}Me)(H_2O)]^-$.[40]

To fit the NMRD profiles at least two rotational correlation times are needed for all dinuclear carbazole compounds. In case of $[Gd_2(L_{carb})(H_2O)_4]^{2-}$ which does not aggregate over the concentration range used in the study either anisotropic overall rotation or internal rotation around the carbazole-DTTA bond can be assigned to the two correlation times. In case of the aggregate forming $[Gd_2(L_{carb\text{-}biphen})(H_2O)_4]^{2-}$ it is difficult to assign the rotational diffusion processes leading to τ_g and τ_l. Aggregates of different size as well as monomers are present in solution. The micelle forming $[Gd_2(L_{carb\text{-}C18})(H_2O)_4]^{2-}$ shows the longest global correlation time τ_R ~ 6 ns. Together with a high order parameter this leads to the highest relaxivities at 30 MHz. Replacing the carbazole by the less rigid biphenylamine does not change relaxivity which allows us to conclude that the rotational behaviour of $[Gd_2(L_{carb\text{-}C18})(H_2O)_4]^{2-}$ and $[Gd_2(L_{bipa\text{-}C18})(H_2O)_4]^{2-}$ micelles is identical. Global rotational correlation times of $[Gd_2(L_{carb\text{-}biphen})(H_2O)_4]^{2-}$ bound to HSA are nearly as long as those of the micelles. Comparison with correlation times obtained for other HSA bound contrast agents is not trivial because often high field relaxivities (ν > 100 MHz) are missing and therefore no analysis is possible using two rotational correlation times.

Table 2. Comparison of water exchange parameters measured on Gd-DTTA complexes

	k_{ex}^{298} (10^6 s^{-1})	$\Delta H^{\ddagger}$ (kJ mol^{-1})	$\Delta S^{\ddagger}$ (J K^{-1} mol^{-1})	
$[Gd_2(L_{carb})(H_2O)_4]^{2-}$	24	58	+90	This work
$[Gd_2(L_{carb\text{-}biphen})(H_2O)_4]^{2-}$	8	36	+8	This work
$[Gd_2(L_{carb\text{-}C18})(H_2O)_4]^{2-}$	8	52	+64	T… w
$[Gd_2(pX(DTTA)_2(H_2O)_4]^{2-}$	9.0	45.4	+41	Re
$[Gd_2(mX(DTTA)_2(H_2O)_4]^{2-}$	8.9	39.2	+20	Re
$[Gd_2(bpy(DTTA)_2(H_2O)_4]^{2-}$	8.1	43.7	+34	Re
$\{Ph_4[Gd(DTTA)(H_2O)_2]^-{}_3\}$	17	39.9	+27	Re
$[Gd(DTTA\text{-}Me)(H_2O)]^-$	24.6	50	+64	Re

CONCLUSION

Several novel compounds based on $[carbazole\text{-}DTTA_2]^{8-}$ h… been synthesized all being able to complex two gadolinium… ions. The carbazole unit has been chosen due to its … structure, the possibility to connect the chelator directly to… aromatic ring and the relatively simple possibility to con… other groups to the carbazole nitrogen. It has been shown … depending on the connected groups the dinuclear compou… can in aqueous solution either build small aggregates, or … aggregate to form micelles or bind non-covalently to proteins… HSA. The slow global rotational diffusion of the micelles for… (τ_g ~6 ns) and the HSA bound complexes (τ_g ~3.2 ns) toge… with the presence of two inner-sphere water molecules per … leads to relaxivities > 40 s^{-1} mM^{-1} (at 30 MHz and 25 … Exchange of the inner-sphere water molecules is fast eno… not to limit relaxivity. By replacing one gadolinium ion by ano… lanthanide the dinuclear carbazole based compounds coul… investigated in view of its used as multimodal imaging agent…

Experimental Section

General: All manipulations were carried out under inert nitrogen atmosphere using standard Schlenk technique unless otherwise mentioned. Human serum albumin (HSA), product number A-1653 (Fraction V Powder 96-99% albumin), was purchased from Sigma Chemical Co. Other reagents and HPLC solvents were supplied by Sigma- Aldrich and Fluka Chemical Co. and were used without further purification.

Compounds 2 and 3 were synthesized and characterized according to Maity et al. [41]. 3,6-Dinitrocarbazole **2** gave a yellow solid (4.4g 70%) as well as 3,6-Diaminocarbazole **3** (0.99 g, 51%.). ^{1}H NMR for **2:** (CD_3CN,

WILEY-VCH
10.1002/ejic.201700847

400MHz) δ in ppm: 7.72 (d, 2H), 8.38 (d, 2H), 9.2 (s, 2H), 10.43 (s, 1H). MS (ESI): 258.2 $[M+1]^+$. ^{1}H NMR for **3:** (DMSO-d6, 400MHz) δ in ppm: 4.11 (s, 4H), 6.72 (d, 2H), 7.17 (s, 2H), 7.18 (d, 2H), 10.18 (s, 1H).

2-[*bis*-(*tert*-butyloxycarbonylmethyl) amino]-ethyl bromide 4 was synthesized according to Achilefu [42]. ^{1}HNMR ($CDCl_3$, 400 MHz) δ in ppm: 1.49 (s, 18H), 3.18 (t, J=8 Hz, 2H), 3.45 (t, J=8 Hz, 2H), 3.5 (s, 4H). MS (ESI) m/z (%): 352.63 (95) $[M+H]^+$.

Tert-butyl 2,2',2'',2''',2'''',2''''',2'''''',2''''''-(2,2',2'',2'''- (9H-carbazole-3,6-diyl) bis (azanetriyl) tetrakis (ethane-2,1-diyl)) tetrakis (azanetriyl) octaacetate 5: 2-[*bis*-(*tert*-butyloxy carbonylmethyl)amino]-ethyl-bromide **4** (1.11 g, 3.15 mmol,), compound **3** (154 mg, 0.78 mmol), and N,N-diisopropylethylamine, (0.83 mg, 6.45 mmol), were refluxed for 36 hours in anhydrous DMF (33 mL) under a nitrogen atmosphere. The solvent was evaporated under vacuum at 40 °C. The crude product was extracted in dichloromethane (2x33 mL) and the organic phase was washed with water (33 mL), then brine (33 mL). The dichloromethane layer was dried over sodium sulfate. The solvent was evaporated under vacuum at 40 °C. Purification of the resulting compound was performed using auto-preparative HPLC model Waters (4.6 × 150 mm Vydac C18) using the gradient mixture of (H_2O 99.89%, HCOOH 0.1%, TFA 0.01%) and (CH_3CN 99.89%, HCOOH 0.1% TFA 0.01%)) (see ESI for more details regarding the gradient concentration). Compound **5** was obtained with 96% purity as a pink solid (0.25 g, 25%). ^{1}H NMR (DMSO-d_6, 400MHz) δ in ppm: 1.38 (s, 72H), 2.75 (t, 8H), 3.34 (t, 8H + s,16H), 6.89 (d, J = 8 Hz, 2H), 7.17 (d, J=8 Hz, 2H), 7.41 (s, 2H), 10.35 (s, 1H). ^{13}C NMR (CD_2Cl_2, 54.00 MHz) δ in ppm: 28.72, 53.20, 57.36, 81.43, 106.75, 112.1, 116.15, 125.19, 135.1, 142.96, 171.38. (ESI): 1283 (33) $[M+H]^+$, 642.25 (100) $[M+2H]^{2+}$.

2,2',2'',2''',2'''',2''''',2'''''',2''''''-((((9H-carbazole-3,6-diyl)bis (azanetriyl))tetrakis(ethane-2,1-diyl))tetrakis(azanetriyl))octaacetic acid 6: The compound **5** (0.12 mmol) was stirred in a mixture of TFA/DCM (50:50 mL), over 24 hours and the reaction monitored by MS (ESI) and/or NMR (tert-butyl peaks disappearance) until completion. The solvents were removed by evaporation, the remaining residue was dissolved in water (10 mL) and the solution was re-evaporated to dryness. This procedure was repeated five times to ensure total loss of acids. H_8L_{carb} was obtained as a pale yellow solid (91 mg, 92 %). ^{1}H-NMR (D_2O= 4.75, 400 MHz) δ in ppm: 3.43 (t, J=8 Hz, 8 H), 3.73 (t, J=8 Hz, 8 H), 3.89 (s, 16 H), 7.42 (d, J=8 Hz, 2 H), 7.60 (d, J=8 Hz, 2 H), 8.03 (s, 2H). MS (ESI-TOF) m/z (%): 417.66 (100) $[M+2H]^{+2}$.

Octa-tert-butyl 2,2',2'',2''',2'''',2''''',2'''''',2''''''-((((9-([1,1'-biphenyl]-4-ylmethyl)-9H-carbazole-3,6-diyl) bis(azanetriyl))tetrakis(ethane-2,1-diyl)) tetrakis(azanetriyl))octaacetate 7: Compound **5** (154 mg, 0.12 mmol) and dry sodium hydride (5.76 mg, 0.24 mmol) were dissolved in dry THF (10 mL) and heated to 70 °C under a nitrogen atmosphere for 2 hours. 4-(bromo-methyl) 1,1'-biphenyl was added to the solution and the mixture was refluxed for 36 hours. Completion of the reaction was monitored by ESI-MS. The solvent was evaporated under vacuum, and the residue was extracted by dichloromethane (CH_2Cl_2/H_2O 30:30 mL). The organic phase was separated and washed with water (30 mL), and then with brine (30 mL). Subsequently the dichloromethane layer was dried over sodium sulfate. The compound **7** was further purified by reverse phase chromatography on a homemade C3 column (see ESI), using a gradient of ACN: H_2O from 60:40 to 90:10%. ^{1}H NMR ($CDCl_3$, 400MHz) δ in ppm: 1.43 (s, 72H), 2.91 (t, 8H), 3.5 (t, 8H), 3.5 (s, 16H), 5.39 (s, 2H), 6.9 - 7.7, (15 ArH). MS (ESI) m/z (%): 724.91 (100) $[M+2H]^{+2}$, 1448.89 (3) $[M+H]^+$.

2,2',2'',2''',2'''',2''''',2'''''',2''''''-((((9-([1,1'-biphenyl]-4-ylmethyl)-9H-carbazole-3,6-diyl)bis(azanetriyl))tetrakis(ethane-2,1-diyl))tetrakis (azanetriyl))octaacetic acid 8: Same procedure than for compound **6,** starting from 0.23mmol (0.33 g) of **7**. $H_8L_{carb\text{-}phen}$ was obtained as a pale yellow solid (0.20 g, 90%). It was not possible to obtain a good ^{1}H NMR for ligand **8** in aqueous solution, possibly due to aggregation. However, disappearance of tert-butyl peaks and observation of broad peaks in the expected aromatic and aliphatic frequency range confirm the complete deprotection reaction. MS (ESI) m/z (%): 1000.0 (15) $[M+H]^+$.

3,6-dinitro-9-octadecyl-9H-carbazole 9: 4,4'-dinitrocarbazole **2** (3.28 mmol, m=2.52 g), 1-bromooctadecane (3.6 mmol, m=1.20 g) and K_2CO_3 (9.8 mmol, m= 1.35g), were dissolved in dimethyformamide and stirred for 36 h at 80 °C. The mixture was allowed to reach room temperature. After addition of water the resulting precipitate was filtered, washed several times with water and dried under reduced pressure. Normal phase chromatography (CH_2Cl_2-MeOH 3%) was performed to obtain the final pure compound as a pale yellow solid (1.13 g, 68 %). ^{1}H NMR ($CDCl_3$ ppm, 400MHz) δ in ppm, 0.88 (t, 3H), 1.23 (m, 30H), 1.93 (m, 2H), 4.42 (t, 2H), 7.53 (dd, J:8 Hz, 2H), 8.48 (dd, J:8 Hz, 2H), 9.27 (s, 2H). MS (ESI) m/z (%): 510.5 $[M+H]^+$.

9-octadecyl-9H-carbazole-3,6-diamine 10: A mixture of **9** (200 0.39 mmol) and 150 mg Pd/C in methanol, was stirred unde atmosphere. The reduction of the nitro groups was monitored by ESI- After completion of the reaction (30 h) the Pd/C was filtered and solvent was removed under reduced pressure. The resulting proc (125 mg) was used in the next step without further purification. ^{1}H N (MeOD, 400MHz) δ in ppm, 0.91 (t, 3H), 1.27 (m, 30), 1.84 (m, 2H), (t, 3H), 7.31 (dd, J:8 Hz, 2H), 7.56 (dd, J:8 Hz, 2H), 7.89 (s, 2H). MS (m/z (%): 450.5 $[M+H]^+$.

Octa-tert-butyl2,2',2'',2''',2'''',2''''',2'''''',2''''''((((9-octadecyl-9Hcarbazole -3,6-diyl) bis(azanetriyl))tetrakis(ethane diyl))tetrakis(azanetriyl)) octaacetate 11: The procedure was simil that of **5**. Compound **4** (2.50 mmol m=0.88g), diisopropylethylamine mmol, m= 0.52 g) and **10** (0.24 g, 0.54 mmol) in 15 mL of anhyd dimethylforamide were refluxed for 16 hours under N_2 atmosphere. work up was identical. The crude product was purified by normal pl chromatography on silica gel with hexane/ ethyl acetate 2:1 (Yield: g, 36%). ^{1}HNMR (CD_2Cl_2=4.85 ppm, 400MHz) δ in ppm 0.85 (t, 3H), (m, 30H), 1.47 (s, 72), 1.72 (m, 2H), 2.92 (t, 8H), 3.49 (s,16), 3.72 (t, 4.25 (t, 2H), 7-7.6 (m, 6H). MS (ESI) m/z (%): 1535.17 (12) $[M+H]^+$, 7 (100) $[M+2H]^{2+}$.

2,2',2'',2''',2'''',2''''',2'''''',2''''''-((((9-octadecyl-9H-carbazole-3,6-diyl)bis(azanetriyl)) tetrakis (ethane-2,1-diyl))tetrakis(azanet octaacetic acid 12: Same procedure than for compound **6,** starting (0.31 g, 0.20 mmol) of **11**. Occasionally ethanol was added to the sol to minimize the formation of foam. (Yield: 0.18g 85%). ^{1}H NMR (Me d4 = 4.87 ppm, 400MHz) δ in ppm 0.86 (t, 3H), 1.25 (m, 30H), 1.8 2H), 2.92 (m, 8H), 3.57 (s, 16H), 3.82 (m, 8H), 4.47 (t, 2H), 7.78 (m, 8.46 (m, 2H). MS (ESI) m/z (%): 1086.83 (11) $[M+H]^+$.

4,4'-Dinitrodiphenylamine 13: The compound was synthes according to a literature procedure [43]. Yield: 2.8 g, 54%. ^{1}HNMR (DM = 2.5 ppm, 400MHz) δ in ppm 7.32 (d, J = 8 Hz, 4H), 8.23 (d, J = 8 4H), 10.0 (s, 1H).

4-nitro-N-(4-nitrophenyl)-N-octadecylaniline 14: The same proce than that for **9** was used, starting from 4,4'-dinitrodiphenylamine (1.9 mmol m=0.51 g), 1-bromooctadecane (0.5 mmol m=0.17 g) and K_2CO_3 (2.0 mmol) to give a pale yellow solid **14** (0.08 g, 31%). ^{1}H NMR (CD_2Cl_2 = 5.32 ppm, 400MHz) δ in ppm: 0.88 (t, 3H), 1.25 (m, 30H), 1.70 (m, 2H), 3.85 (t, 2H), 7.14 (d, 4H), 8.18 (d, 4H).

N1-(4-aminophenyl)-N1-octadecylbenzene-1,4-diamine 15: The same procedure than that for **10** was used, starting from **14** (55 mg, 0.11 mmol) and 50mg Pd/C in methanol. Compound **15** (29 mg, 58%) was used in the next step without further purification. ^{1}HNMR ($CDCl_3$, 400 MHz) δ in ppm: 0.86 (m, 3H), 1.25 (s, 30H), 3.5 (t, 2H), 3.33-3.52 (broad band, 4H), 6.61 (dd, 4H), 6.74 (dd, 4H). MS (ESI) m/z (%): 452.6 (100) $[M+H]^+$.

WILEY-VCH
10.1002/ejic.201700847

Octa-tert-butyl 2,2',2'',2''',2'''',2''''',2'''''',2'''''''-(((((octadecylazanediyl) bis (4,1-phenylene))bis(azanetriyl))tetrakis(ethane-2,1-diyl))tetrakis (azanetriyl))octaacetate 16: The procedure was similar to that of **11**. Compound **16** was obtained as a pale yellow solid (0.14 g, 18.2 %). ^{1}H NMR (CD_2Cl_2, 400MHz) δ in ppm 0.83 (t, 3H), 1.29 (s, 30), 1.49 (s,72 H), 2.80 (t, 8H), 3.42 (t, 8H), 3.48 (s, 16H), 6.68 (dd, 4H), 6.79 (dd, 4H). MS (ESI) m/z (%): 1537.0 (26) $[M+H]^+$, 769.42 (100) $[M+2H]^{2+}$.

2,2',2'',2''',2'''',2''''',2'''''',2'''''''-(((((octadecylazanediyl) bis (4,1-phenylene)) bis(azanetriyl))tetrakis(ethane-2,1-diyl))tetrakis (azanetriyl))octaacetate 17: The procedure was similar to that of **12**. Compound **17** was obtained as a pale yellow solid (89mg, 90 %). ^{1}H NMR spectrum of the compound **17** shows broad peaks due to aggregation in solution. MS (ESI) m/z (%): [M] (15 %) 1087.

Preparation of gadolinium complexes: A solution of $GdCl_3$ in water was prepared and the exact concentration of Gd^{3+} was measured by bulk magnetic susceptibility (BMS) [44] at 21.2 °C on a Bruker DRX-400 (9.4 T, 400 MHz). For preparation of $[Gd_2(L_{carb})(H_2O)_4]^{2-}$, H_8L_{carb} **(6)** was dissolved in water at room temperature and it's concentration was determined by back titration of a Gd^{3+} excess with Na_2H_2EDTA (0.022 mM) using a Metrohm 665 Dosimat for titration (indicator: xylenol orange). The final complexation with Gd^{3+} was performed with a small excess of ligand (3%). The pH was adjusted to 5.9 with NaOH (0.05 M). Absence of free Gd^{3+} was checked by the xylenol orange test [45]. After complexation, the exact concentration of Gd^{3+} was measured by BMS, $[Gd^{3+}]$ = 4.01 mM. Preparation of the other complexes was performed by the same way. Gadolinium concentrations as measured by BMS were Gd^{3+} = 0.66 mM for $[Gd_2(L_{carb\text{-}biphen})(H_2O)_4]^{2-}$, 2.16 mM for $[Gd_2(L_{carb\text{-}C18})(H_2O)_4]^{2-}$ and 1.15 mM for $[Gd_2(L_{bipa\text{-}C18})(H_2O)_4]^{2-}$.

Preparation of 12% (w/v) HAS: HSA was dissolved in 50 mM HEPES buffer. A molecular weight of 66435 Da was taken to estimate the concentration. The pH of the final solution was adjusted to 7.4 using NaOH 0.1 mM. The precise concentration of protein was obtained by UV-Vis as 1.62 mM (see ESI).

Binding $[Gd_2(L_{carb\text{-}biphen})(H_2O)_4]^{-2}$ to human serum albumin (HSA): An appropriate amount of 12% (w/v) HSA was added to 600 µl of a solution 0.66 mM of $[Gd_2(L_{carb\text{-}biphen})(H_2O)_4]^{2-}$ to have the final ratio of [HSA] / $[Gd_2(L_{carb\text{-}biphen})(H_2O)_4]^{2-}$ = 3.9. The final concentration of HSA w ~4.5% is about the concentration in plasma. The pH of the solution was adjusted to 7.4 and the concentration of Gd^{3+} in the HSA solution was determined by ICP-OES (Optima 2000 spectrometer, Perkin-Elmer; $[Gd^{3+}]$ = 77 µM).

^{1}H relaxivities: ^{1}H NMRD profiles were obtained on a Stelar Spinmaster fast field cycling NMR relaxometer (2.35×10^{-4} to 0.47 T; proton Larmor frequencies 0.01-20 MHz) equipped with a VTC90 temperature control unit, on Bruker minispecs (0.71 T (30 MHz), 0.94 T (40 MHz), and 1.41 T (60 MHz), on a Bruker Avance-200 console connected to 2.35 T (100 MHz) and 4.7 T (200 MHz) cryomagnets, and on a Bruker Avance-II 9.4 T (400 MHz). All temperatures were measured by substitution techniques.[46]

^{17}O NMR: Variable- temperature ^{17}O NMR measurements were performed on a Bruker Avance-II 9.4 T (54.3 MHz) spectrometer equipped with a Bruker BVT3000 temperature control and a Bruker BCU05 cooling unit. The ^{17}O relaxation rates were measured at variable temperature in the range of 278-345 K. ^{17}O-enriched water (Irakli Gverdtsiteli Research and Technology Center on High Technologies and Super Pure Material LTD) was added to the samples to have a final 2% ^{17}O enrichment to improve sensitivity. The final Gd^{3+} concentration of the samples containing a carbazole $[Gd_2(L_{carb})(H_2O)_4]^{2-}$ and a biphenyl-carbazole $[Gd_2(L_{carb\text{-}biphen})(H_2O)_4]^{2-}$ were 11.25 and 0.63 mM, respectively. The samples were sealed in glass spheres adapted for 10 mm NMR tubes to avoid susceptibility corrections to the chemical shifts [47]. Transverse ($1/T_2$) and longitudinal ($1/T_1$) relaxation rates were measured using the inversion recovery [48] and the Carr-Purcell-Meiboom-Gill pulse sequences [49], respectively.

Data Analysis: The simultaneous least squares fits of the ^{1}H NMRD, ^{17}O NMR and the determination of the HSA-ligand binding affinity constant were carried out using the programs Visualizeur/Optimiseur running on a Matlab platform, version 7.6.0 (R2008).[50]

Acknowledgments

MM and LH acknowledge financial support from the Swiss National Science Foundation.

Keywords: Gadolinium • Imaging agents • Chelates • Dinuclear complexes • Aggregation

[1] P. A. Rinck, *Magnetic Re-so-nan-ce in Me-di-ci-ne. The E Textbook of the European Magnetic Resonance Forum.*, Euro Magnetic Resonance Forum, Www.magr Resonance.org/Contents.html, **2017**.
[2] S. Laurent, L. Vander Elst, R. N. Muller, *Contrast Media Mol. Ima* **2006**, *1*, 128–137.
[3] C. F. G. C. Geraldes, S. Laurent, *Contrast Media Mol. Imaging* **200** 1–23.
[4] L. Helm, *Future Med. Chem.* **2010**, *2*, 385–396.
[5] L. Helm, *Chimia* **2011**, *65*, 696–698.
[6] V. C. Pierre, M. J. Allen, P. Caravan, *J. Biol. Inorg. Chem.* **2014** 127–131.
[7] P. Caravan, J. J. Ellison, T. J. McMurry, R. B. Lauffer, *Chem. Rev.* **1** *99*, 2293–2352.
[8] P. Caravan, *Chem. Soc. Rev.* **2006**, *35*, 512–523.
[9] S. Aime, S. G. Crich, E. Gianolio, G. B. Giovenzana, T. L., E. Ter *Coord. Chem. Rev.* **2006**, *250*, 1562–1579.
[10] D. H. Powell, O. M. Ni Dhubhghaill, D. Pubanz, L. Helm, Y. S. Lebe W. Schlaepfer, A. E. Merbach, *J. Am. Chem. Soc.* **1996**, *118*, 9 9346.
[11] W. Li, S. E. Fraser, T. J. Meade, *J. Am. Chem. Soc.* **1999**, *121*, 1 1414.
[12] W. Li, G. Parigi, M. Fragai, C. Luchinat, T. J. Meade, *Inorg. C* **2002**, *41*, 4018–4024.
[13] J. Costa, É. Tóth, L. Helm, A. E. Merbach, *Inorg. Chem.* **2005** 4747–4755.
[14] T. N. Parac-Vogt, K. Kimpe, S. Laurent, L. Vander Elst, C. Burte Chen, R. N. Muller, Y. Ni, A. Verbruggen, K. Binnemans, *Chem. E* **2005**, *11*, 3077–3086.
[15] J. Costa, E. Balogh, V. Turcry, R. Tripier, M. Le Baccon, F. Chul H. Handel, L. Helm, E. Tóth, A. E. Merbach, *Chem. Eur. J.* **2006** 6841–6851.
[16] A. Mishra, P. Fousková, G. Angelovski, E. Balogh, A. K. Mishra, Logothetis, É. Tóth, *Inorganic Chemistry* **2008**, *47*, 1370–1381.
[17] G. Zhao, C. Lu, H. Li, Y. Xiao, W. Zhang, X. Fang, P. Wang, X. F J. Xu, W. Yang, *Inorg. Chim. Acta* **2013**, *406*, 146–152.
[18] A. Fontes, S. Karimi, L. Helm, M. Yulikov, P. M. Ferreira, J. P. André, *Eur. J. Inorg. Chem.* **2015**, 1579–1591.
[19] J. B. Livramento, A. Sour, A. Borel, A. E. Merbach, É. Tóth, *Chem. Eur. J.* **2006**, *12*, 989–1003.
[20] J. B. Livramento, L. Helm, A. Sour, C. O'Neil, A. E. Merbach, É. Tóth, *Dalton Trans.* **2008**, 1195–1202.
[21] L. Moriggi, A. Aebischer, C. Cannizzo, A. Sour, A. Borel, J.-C. G. Bünzli, L. Helm, *Dalton Trans.* **2009**, 2088–2095.
[22] H. Jaccard, P. Miéville, C. Cannizzo, C. R. Mayer, L. Helm, *JBIC* **2014**, *19*, 145–159.
[23] F. A. Dunand, A. Borel, A. E. Merbach, *J. Am. Chem. Soc.* **2002**, *124*, 710–716.

[24] F. Yerly, A. Borel, L. Helm, A. E. Merbach, *Chem. Eur. J.* **2003**, *9*, 5468–5480.
[25] G. Angelovski, I. Mamedov, *Curr. Inorg. Chem.* **2011**, *1*, 76–90.
[26] G. Lipari, A. Szabo, *J. Am. Chem. Soc.* **1982**, *104*, 4546–4559.
[27] G. Lipari, A. Szabo, *J. Am. Chem. Soc.* **1982**, *104*, 4559–4570.
[28] F. A. Dunand, É. Tóth, R. Hollister, A. E. Merbach, *J. Biol. Inorg. Chem.* **2001**, *6*, 247–255.
[29] D. Nie, Z. Chen, Z. Bian, J. Zhou, Z. Liu, F. Chen, Y. Zhao, C. Huang, *New J. Chem.* **2007**, *31*, 1639.
[30] N. S. Baek, Y. H. Kim, Y. K. Eom, J. H. Oh, H. K. Kim, A. Aebischer, F. Gumy, A.-S. Chauvin, J.-C. G. Bünzli, *Dalton Trans.* **2010**, *39*, 1532–1538.
[31] J. Wang, C. Han, G. Xie, Y. Wei, Q. Xue, P. Yan, H. Xu, *Chem. Eur. J.* **2014**, *20*, 11137–11148.
[32] T. Yu, R. Liang, Y. Zhao, Y. Song, B. Gao, M. Li, L. Min, H. Zhang, D. Fan, *Polyhedron* **2015**, *85*, 789–794.
[33] G. M. Nicolle, É. Tóth, K.-P. Eisenwiener, H. R. Mäcke, A. E. Merbach, *J. Biol. Inorg. Chem.* **2002**, *7*, 757–769.
[34] L. Helm, *Prog. NMR Spectroscopy* **2006**, *49*, 45–64.
[35] É. Tóth, L. Helm, A. E. Merbach, in *The Chemistry of Contrast Agents in Medical Magnetic Resonance Imaging* (Eds.: A.E. Merbach, L. Helm, É. Tóth), John Wiley & Sons Ltd., Chichester, **2013**, pp. 25–82.
[36] R. N. Muller, B. Radüchel, S. Laurent, J. Platzek, C. Piérart, P. Mareski, L. Vander Elst, *Eur. J. Inorg. Chem.* **1999**, 1949–1955.
[37] P. Caravan, N. J. Cloutier, M. T. Greenfield, S. A. McDermid, S. U. Dunham, J. W. M. Bulte, J. C. J. Amedio, R. J. Looby, R. M. Supkowski, W. D. Horrocks, et al., *J. Am. Chem. Soc.* **2002**, *124*, 3152–3162.
[38] S. Aime, E. Gianolio, D. Longo, R. Pagliarin, C. Lovazzano, M. Sisti, *ChemBioChem* **2005**, *6*, 818–820.
[39] S. Torres, J. A. Martins, J. P. André, C. F. G. C. Geraldes, A. E. Merbach, É. Tóth, *Chem. Eur. J.* **2006**, *12*, 940–948.
[40] S. Karimi, G. Hunter, L. Moriggi, C. Platas-Iglesias, L. Helm, *Inorg. Chem.* **2016**, *55*, 6231–6239.
[41] S. C. Maity, D. Mal, M. M. Maiti, *Thermochimica Acta* **2005**, *435*, 135–141.
[42] S. I. Achilefu, *Versatile Method for the Synthesis of Diethylenetriaminepentaacetic Acid Esters.*, **2001**, WO 2001002339.
[43] Y. J. Joo, J.-E. Kim, J.-I. Won, K.-U. Hwang, *Preparation of 4,4'-dinitrodiphenylamine from Urea and Nitrobenzene.*, **2001**, 2001040161.
[44] D. M. Corsi, C. Platas-Iglesias, H. Van Bekkum, J. A. Peters, *M Reson. Chem.* **2001**, *39*, 723–726.
[45] M. Randin, G. Brunisholz, *Helv. Chim. Acta* **1959**, *42*, 1927–1938.
[46] C. Ammann, P. Meier, A. E. Merbach, *J. Magn. Reson.* **1982**, *46*, 321.
[47] A. D. Hugi, L. Helm, A. E. Merbach, *Helv. Chim. Acta* **1985**, *68*, 521.
[48] R. L. Vold, *J. Chem. Phys.* **1972**, *56*, 3210–3216.
[49] S. Meiboom, D. Gill, *Rev. Sci. Instrum.* **1958**, *29*, 688–691.
[50] F. Yerly, *VISUALISEUR/OPTIMISEUR*, EPFL, Lausanne, **2003**.